



Role of Kruppel-like Factor 2 in Intracranial Aneurysm of the Rabbit Model

X. Wu¹, J. Zhang², Q. Huang¹, P. Yang¹, J. Chen¹ and J. Liu¹

¹ Department of Neurosurgery, Changhai Hospital, Shanghai, China 200433

² Department of Neurosurgery, PLA 455 Hospital, Shanghai, China 200052

Corresponding author: Dr. Qinghai Huang and Dr. Jianmin Liu, Department of Neurosurgery, Changhai Hospital, 168 Changhai Road, Yangpu district, Shanghai, China 200433. E-mail: qinghai_huang@yeah.net and ljmjianmingliu@126.com

Abstract

We investigated expression of Kruppel-like factor 2 (KLF2) and its correlation with basilar artery blood flow rate in the hemodynamically induced aneurysm model built by different methods. New Zealand rabbits were randomly divided into sham-operated group, unilateral ligation of common carotid artery (CCA) group (UL group) and bilateral ligation of CCA group (BL group). Rabbits were cervix-cut to expose the arteries without ligation (sham group), with right-side ligation (UL group) and bilateral ligation (BL group), respectively. Skull Doppler ultrasound was used to measure basilar artery blood flow rate in each group at week 1, 2, 3, or 4 separately (n=6 for each time point). The animals were killed after the measurements. At each time point, 6 basilar artery bifurcates from each group were collected and sent for staining (HE, EVG, Masson and KLF2 immunohistochemistry staining), while another 6 basilar artery bifurcates were processed with KLF2 Western blotting. Results showed that the average blood flow rate did not change significantly among the 4 time points in the Sham group, but it was insignificantly smaller compared to the UL group. The average blood flow rate in the BL group was significantly higher than that in the other two groups. Pathological tests showed that according to the aneurysm evaluation criteria, the basilar arteries in the Sham group had smooth tip lumina, complete endothelial cells, complete internal elastic membranes, but no fracture, thinning or aneurysm formation. Only 1 of 24 rabbits in the UL group had slight bulges in the tip of basilar artery, though not very severe. Twelve rabbits in the BL group had aneurysmal bulges, significantly different from the other two groups. KLF2 protein expression was not changed significantly with time in the Sham group, but increased slightly with time in the UL group. KLF2 protein expression in the BL group increased significantly only after 1 week and then maintained a high level, significantly different from the other two groups. KLF2 protein expression was positively correlated with blood flow rate. In conclusion, the hemodynamic change was most significant after bilateral ligation, which was most suitable for building animal models for aneurysm research. And KLF2 expression change was consistent with blood flow rate variation, which showed positive correlation, indicating KLF2 expression was regulated by hemodynamic changes.

Key words: Kruppel-like factor 2, Hemodynamics, Basilar artery, Aneurysm, Rabbit Model.

Introduction

Kruppel-like factor 2 (KLF2) is a member of the Kruppel-like factor family of zinc finger transcription factors, and it has been implicated in a variety of biochemical processes in the human body, including lung development, embryonic erythropoiesis, epithelial integrity, T-cell viability, and adipogenesis(1). KLF-2 is a pivotal in maintaining the development of endothelial cells and the normal structure and functions of blood vessels (2). Most importantly, KLF2 can be regulated by intravascular wall shear stress (WSS), corresponding to the change of its expression. Pulsed blood flow can increase KLF2 expression via the ERK5/MEF2 (extracellular signal-regulated kinases5/myocyte enhancer factor 2) pathway, and reduce the KLF2 expression by inhibiting the Src pathway (3). And KLF2 regulates expression of several inflammatory factors, such as VCAM-1(vascular cell adhesion molecule 1), E-selectin and NF- κ B (nuclear factor kappa-light-chain-enhancer of activated B cells)(4). However, KLF2 is a central regulator of endothelial and monocyte/macrophage proinflammatory action (5, 6). Although the effects of KLF2 in macrophage activation predict that it likely inhibits vascular inflammation, the function of KLF2 in this process remain uncertain.

The formation of intracranial aneurysm (ICA) is closely related to hemodynamic variation. So far, there are several hemodynamically induced aneurysm models. In

a unilateral or bilateral common carotid artery (CCA) ligation rabbit model, the compensatory increment of posterior circulation of basilar artery blood flow induces the formation of aneurysm on the basilar artery tip. This model, which only has hemodynamic variation and excludes interferences from blood pressure elevation or angiotensin, is most suitable to investigate the pathological mechanism of aneurysm.

Moreover, the difference of basilar artery tip blood flow between unilateral and bilateral ligations provides a meaningful basis to evaluate the change of KLF2 following hemodynamic variation. Here we found the hemodynamically induced cerebral artery aneurysm model by a CCA ligation method. The rabbits were observed at week 1, 2, 3, or 4 after ligation (n=6 for each time point), and basilar artery blood flow rate was measured. Then the rabbits were sacrificed via heart perfusion. Samples were collected immediately and sent for pathological examination of basilar artery changes. Meanwhile, immunohistochemical examination and Western blot were performed to detect KLF2 in the basilar artery. This study aimed to investigate the relationship between hemodynamic changes and KLF2.

Materials and methods

Experimental animals

All animals were supplied by the Laboratory animal center of The Second Military Medical Universi-

ty, Shanghai, RP China. A total of 144 four-month-old male New Zealand rabbits (2.0-2.5 kg) were enrolled in the study, and all animal experiments were performed in accordance to the guidelines established by the Animal Care and Experimentation Committee of The Changhai Medical Research Institute, and all experimental protocol were approved by the Experimentation Committee of The Changhai Medical Research Institute. The rabbits were randomly divided into three groups, namely sham group, unilateral ligation of CCA group (UL group), and bilateral ligation of CCA group (BL group) (n=48 for each group). Animals in each group were tested at week 1, 2, 3 or 4 after ligation (n=6 for each time point).

The aneurysm model of the rabbit induced hemodynamically

The animals were anaesthetized with 0.2 ml/kg xylazine hydrochloride (Sigma, USA) solution by intramuscular injection, and after quietness, 1% pentobarbital sodium (Sigma, USA) (20 mg/kg) was injected via the ear vein until eyelash reflex disappeared. After anesthesia, the four limbs, in the dorsal position, were fixated onto a small animal fixation station. The hair from suprasternal fossa to the middle of lower-jaw horizontal neck was shaved, followed by iodophor disinfection solution and hole towel spread to the rabbit. At the cervical median incision, the skin in front of the trachea was cut open, and the muscles in anterior cervical region were cut wide along the neck white line until reaching the trachea. The neck muscles were opened and separated at the lateral trachea, exposing the bilateral CCAs. Then the cervical arterial sheath was separated, and the cervical arteries were stripped off, without injury of the vagus. Rabbits were treated without ligation (Sham group), with right-side ligation (UL group) (Fig. 1A) and with bilateral ligations (BL group), respectively (Fig. 1B). After the ligation, the wounds were sewed up. After the anesthesia disappeared, the animals were returned to the cages at heat preservation, and free to food and water. Their behaviors were observed.

Measurement of basilar artery flow rate

Skull Doppler ultrasound was used to measure basilar artery blood flow rate at week 1, 2, 3, or 4 after operation. In the prone position of arteries, a soft pillow was padded under the cervix. The head was bent forwards to expose the occiput. Scan detection via an ultrasound probe was performed from the occiput in parallel to the basilar artery to measure the maximum flow rate.

Specimen acquisition and pathological examination

With the same anesthesia method, 1% pentobarbital sodium was provided at a dose of 40 mg/kg to ensure deep anesthesia. After that, the four limbs, at the dorsal position, were fixated into a small animal fixation station. The chest was opened in a U-form from behind the xiphisternum to the two sides. The pericardium was clipped open to expose the heart. An infusion needle penetrated through the ventricular walls to the left ventricle, with fixed by a vascular clamp. The perfusion infusion switch was opened with good dripping, so the right auricle was clipped open. Also the blood circulation in the inferior vena cava was blocked. First 500 ml of 4 °C normal saline and then 4% paraformaldehyde

(PFA) were perfused within more than 30 min, which ensured full fixation of the tissues. After craniotomy, the complete basilar artery and brain stem were taken down. The tip bifurcation at the basilar artery was intercepted down, and fixed by PFA in the middle and posterior part. After 72 h, the specimens were paraffin-embedded and sliced. The specimens for Western blot analysis were not treated with PFA perfusion or after-fixation. Then the basilar arteries were taken down, quickly frozen with liquid nitrogen, and stored in a -80 °C refrigerator.

Histological observation

The tip bifurcation was fixed by PFA for 72 h and then paraffin-embedded. The specimens were sliced with a longitudinal cutting method so that the bilateral posterior cerebral arteries were in the same plane as the basilar artery trunk, and the knife face was in parallel to this plane. The objective was to expose the lumina at the basilar artery tip bifurcation, which was favorable for observing the formation site and shape of aneurysm. The paraffin sections (6 µm thick) were stained by hematoxylin-eosin (HE), elastica van Gieson (EVG), Masson and immunohistochemical (IHC) method. Sections of paraffin embedded tip bifurcation tissue were deparaffinized and rehydrated. Endogenous peroxidase activity was blocked with 0.3% hydrogen peroxide, diluted in PBS (pH 7.4), for 10 min. After rinsing three times in PBS (3 min each), sections were incubated with 5% normal goat serum at room temperature for 20 min to block the non-specific binding sites, and then incubated overnight at 4°C in the presence of primary polyclonal antibodies (mouse anti-KLF-2, Abcam, US) diluted 1:100 in PBS. To control for non-specific staining, the primary antibodies were replaced with normal PBS. The sections were then rinsed in PBS (3 min) and incubated with the secondary antibody (polymerized HRP conjugated goat-anti mouse IgG) (Zhongshan Golden Bridge, China) at 37°C for 30 min, and then washed 3 times in PBS (5 min each). Immunoreactivity was then visualized by incubating the sections in 3,3'-diamino-benzidine (DAB) substrate. The sections were then counterstained with hematoxylin and coverslips were sealed with neutral balsam. Sections were examined using a Leica DMIRB (Leica, Wetzlar, Germany) computerized microscope with a Leica digital camera DFC320 attachment, and images were captured and stored for analysis.

Analysis of KLF2 protein expressions by Western blot

After basilar artery bifurcation was treated by differentiation protocol, the total proteins from tissues extracts were prepared and protein concentrations were measured using a Bradford assay (Biorad) and equal amounts of protein were subjected to sodium dodecyl sulfate polyacrylamide gel electrophoresis (SDS-PAGE) and western transfer onto PVDF membranes, which were blocked 1 hour at RT in blocking buffer (5% nonfat dried milk, 10 mM Tris pH 7.5, 100 mMNaCl, and 0.1% Tween 20, TBST) and washed. The primary antibody was used at 1:1000 in TBST buffer overnight at 4°C. Horseradish peroxidase-labeled (HRP) secondary antibody (Santa Cruz biotechnology) was used at 1:3000 and blots were developed using ECL Plus (Thermo Fisher Scientific Inc, New York, USA).

Table 1. Average basilar artery blood flow rates ($\bar{x}\pm s$)

Group	At 1W	At 2W	At 3W	At 4W
Sham	37.45±4.26	39.97±4.92	37.10±7.88	46.07±7.80
UL	63.50±7.41	51.35±7.81	54.56±5.25	61.56±14.94
BL	89.18±7.64	101.71±16.56	69.25±8.68	89.65±7.08

Statistical Analysis

Statistical analyses of the data were performed with a one-way ANOVA followed by the Tukey-Kramer honestly significant difference (HSD) test for the three sets of results. A P-value of less than 0.05 was considered significant. Statistical analyses were done with a JMP® Statistical Discovery Software (SAS Institute, Cary, NC).

Results

The blood flow rate of basilar artery

The blood flow rate in the Sham group did not change significantly at the four time points. The blood flow rate in the UL group increased slightly with time, but the change was not significant compared to the Sham group. The blood flow rate in the BL group increased significantly after week 1, maximized at week 2, and maintained at a high level afterwards. The change were

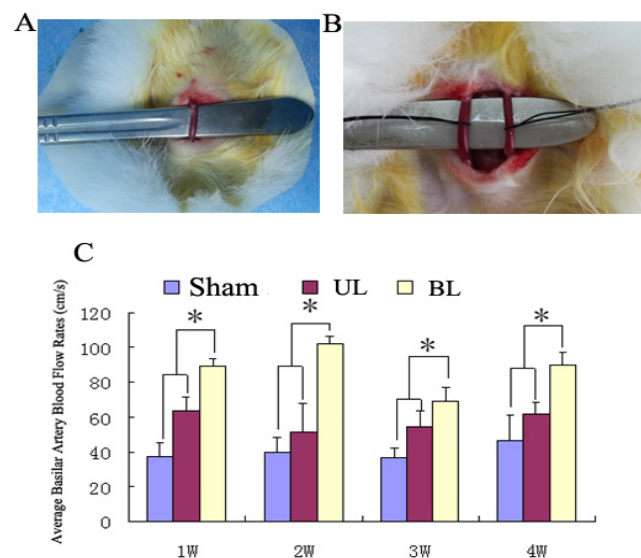


Figure 1. Aneurysm model of rabbit induced by hemodynamically. A Unilateral (right-side) ligation of CCA; B Bilateral ligation of CCA; C Average basilar artery blood flow rates at different time points. The blood flow rates in the BL group versus the other two groups are significantly larger.

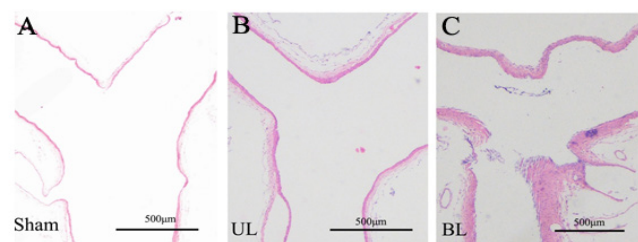


Figure 2. Observation of vascular coronary slices at basilar artery bifurcation. A Sham: The lumina at the bifurcation have smooth sections, without obvious bulging. B UL: The bifurcations show continuous endothelial cells, without lumen bulges, because of the compensatory expansion of right posterior cerebral artery tubes due to the hemodynamic effect after right-side ligation. C BL: The basilar artery tips are bulging, with thinning of local walls.

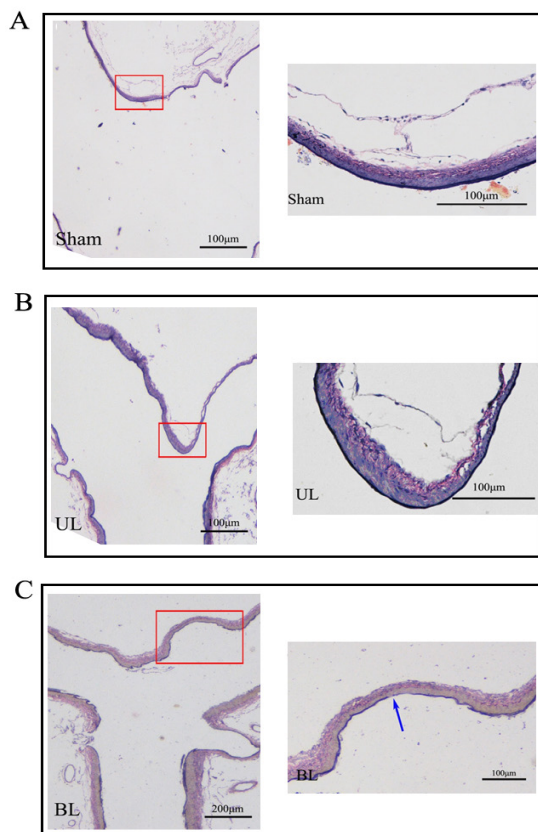


Figure 3. EVG staining of basilar artery. A (Sham): EVG staining shows smooth internal elastic membranes at the bifurcation, without thinning or deletion. B (UL): EVG staining shows smooth internal elastic membranes at the bifurcation, without thinning or deletion. C (BL): EVG staining shows local thinning and deletion of internal elastic membranes (blue arrowhead), with local bulging, thinned middle-layer smooth muscles, which accord with the pathological changes of aneurysm.

significant compared to the other two groups ($p<0.05$). The results are listed in Table 1 and Fig. 1 C. Histological observation of basilar artery in different groups were showed in Fig. 2 using HE staining.

Basilar tip aneurysm-like bulges

According to aneurysm-like bulge evaluation criterion, the internal elastic force was evaluated by EVG staining (Fig. 3), and smooth muscles were assessed by Masson staining (Fig.4). The basilar arteries in the Sham group had smooth tip lumina, complete endothelial cells and complete internal elastic membranes, but no fracture, thinning or aneurysm formation. Only 1 of 24 rabbits in the UL group had slight outward bulging, though it was not very severe in the tip of basilar artery. Twelve rabbits in the BL group had aneurysmal bulges. The aneurysm formation conditions in the three groups are significantly different (Table 2, $*p<0.05$).

KLF2 IHC staining

In the Sham group, a part of endothelial cells in basilar artery tips were weakly stained, but scattered positive staining occurred in the middle-layer smooth muscle cells, and a small amount of positive staining occurred in some dispersed cells in vascular adventitia (Fig. 5). In the UL group, besides the enhanced expression in the inner-layer cells, positive staining also appeared in the middle-layer smooth muscle cells (Fig. 6). In the BL

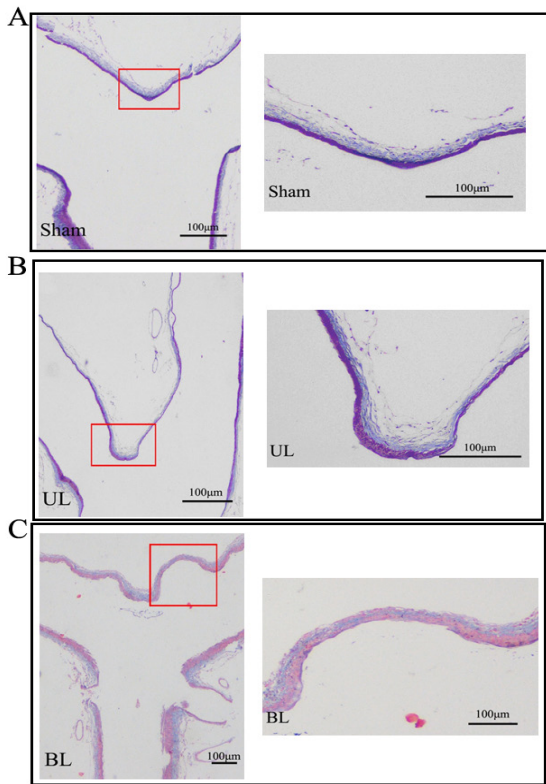


Figure 4. Masson staining of basilar artery. A (Sham): Masson staining shows uniform thickness of middle-layer smooth muscles in the bifurcation, without significant thinning. B (UL): Masson staining shows uniform thickness of middle-layer smooth muscles in the bifurcation, with slight local thinning. C (BL): Masson staining shows swelling of middle-layer smooth muscles in the bifurcation, with thinning at the tip.

Table 2. Aneurysm formation in basilar artery.

Group	At 1W	At 2W	At 3W	At 4W
Sham	0	0	0	0
UL	0	0	1	0
BL	2	2	4	4

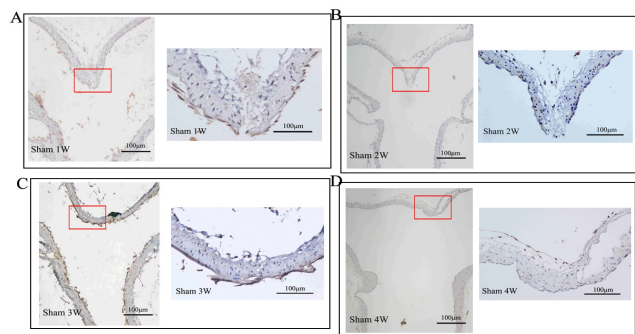


Figure 5. Basilar artery KLF2 IHC staining in the Sham group. A: Sham-1W; B: Sham-2W; C: Sham-3W; D: Sham-4W. KLF2 positive staining mainly appears in endothelial cells for all subgroups, while the middle-layer smooth muscle cells are positively-stained in a scattered way, showing no significant difference among subgroups.

group, KLF2 was strongly expressed in all layers with time extension, and it was significant compared to the other two groups (Fig. 7). The proportion of positive cells in all groups is listed in Table 3 and Fig. 8.

Western blot

The Western blot (Fig. 9) showed that with time increased the level of KLF2 proteins was not significantly changed in Sham group; KLF2 level in the UL group

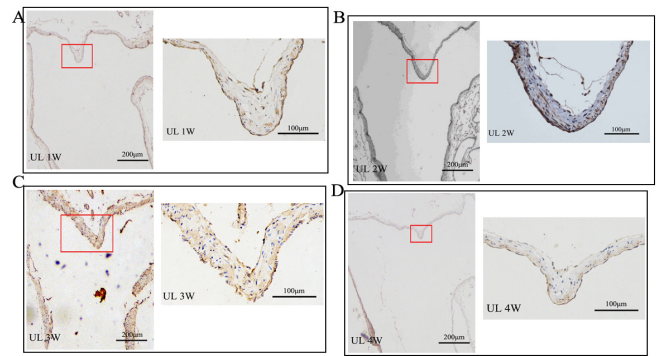


Figure 6. Basilar artery KLF2 IHC staining in the UL group. A: UL-1W; B: UL-2W; C: UL-3W; D: UL-4W. KLF2 is strongly expressed since 1W, mainly in endothelial cells and smooth muscle cells, showing no significant differences among four subgroups. The proportions of positive cells are smaller versus the BL group. UL= unilateral ligation.

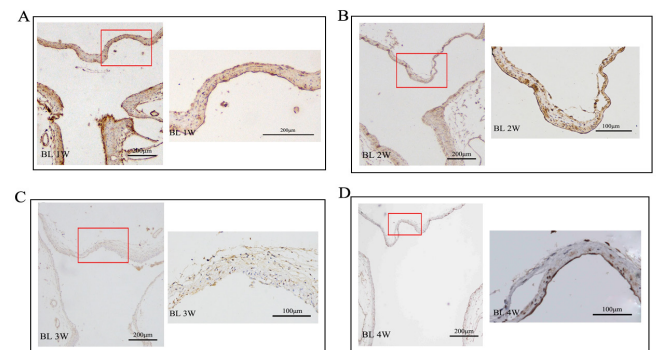


Figure 7. Basilar artery KLF2 IHC staining in the BL group. A: BL-1W; B: BL-2W; C: BL-3W; D: BL-4W. KLF2 is strongly expressed since week 1; besides endothelial cells, its expression proportion is also significantly increased in the middle-layer smooth muscle cells, showing no significant differences among four subgroups. BL=Bilateral ligation.

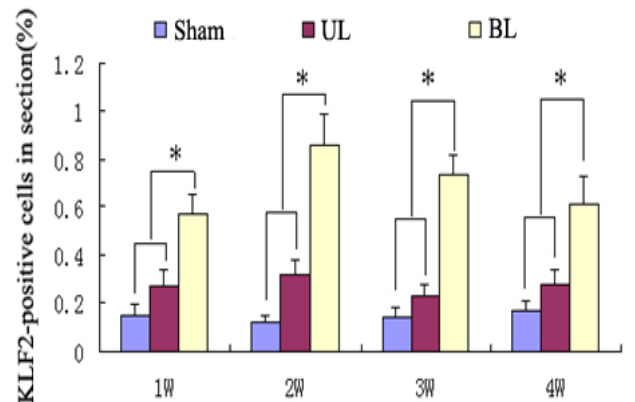


Figure 8. Proportions of positive cells with KLF2 IHC staining in basilar artery tips. The proportions of positive cells increase gradually: Sham < UL < BL; the proportions are significantly highest in the BL group (P<0.01).

Table 3. Proportions of positive cells with KLF2 IHC staining in basilar artery tips.

Group	At 1W	At 2W	At 3W	At 4W
Sham	0.15± 0.05	0.12± 0.03	0.14± 0.04	0.17± 0.04
UL	0.27± 0.07	0.32± 0.06	0.23± 0.05	0.28± 0.06
BL	0.52± 0.09	0.86± 0.13	0.74± 0.08	0.62± 0.11

increased slightly with time, but KLF2 level in the BL group significantly increased since week 1 and maintained a high level afterwards(P<0.05).

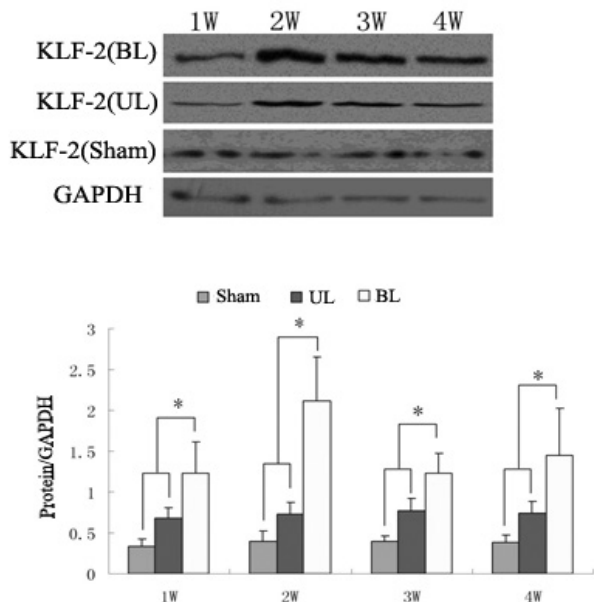


Figure 9. KLF2 protein expressions in basilar arteries of all groups. A protein expression of KLF2 in basilar arteries at different time points. B Quantification of KLF2 in different groups, *: $P < 0.05$.

Correlations between hemodynamic changes and KLF2 protein expressions

The blood flow rate after CCA ligation increased mostly significantly in the BL group, with the corresponding rise of aneurysm formation rate. Accordingly, KLF2 protein levels were improved with the rise of blood flow rate. Correlation analysis showed that there was a remarkable negative correlation ($r = 0.845$, $P < 0.05$).

Discussion

So far, the pathogenesis of ICA is poorly understood (7). It is believed that its occurrence and development are related to many factors, such as genetic factors, acquired living environment, smoking, and hypertension (8). Many researchers find that ICA mostly occurs at vascular bifurcations or the tangent line of vascular bulges (9-11). Clinical studies show that the incidence of aneurysm increases in patients with rise of local intracranial blood flow due to carotid obstruction and those with intracranial arteriovenous malformation blood supply (12). Such aneurysm formation is related to the significant increase of blood flow in tumor-carrying vessels (13). It is thus believed that hemodynamic variation is a major risk factor inducing the aneurysm formation (14). Studying causality between hemodynamics and aneurysm formation in humans is very difficult, which only depends on reliable hemodynamically induced aneurysm animal models.

An ideal aneurysm model with pure hemodynamic induction requires conditions that its pathogenesis is identical to the occurrence mechanism of human aneurysm, and the cerebrovascular hemodynamics can be quantitatively analyzed. So far, there is no cerebral aneurysm model that is consistent with the occurrence mechanism of human aneurysm and satisfies the requirements of research on pathology and hemodynamics. The existing methods for aneurysm modeling include

vein pouch suture, vascular anastomosis, and elastic enzyme injection. The models built from the first two methods are pathologically very different from the true human ICAs, while those built from the third method are more like human true aneurysms in terms of general pathology, proteins and gene expressions. However, such aneurysms are located at the cervix and aorta of animals, which are significantly different from intracranial vascular structure in terms of vascular walls, and the intracranial vessels are dominated by an inner elastic layer, but the middle-layer smooth muscles and vascular adventitia are too thin. Moreover, because of large difference between the surrounding environment and human ICA, it is surrounded by soft tissues rather than a subarachnoid space surrounding non-ICAs, thus the pathologic process of spontaneous rupture bleeding is hard to simulate. Here we used New Zealand rabbits and built aneurysm models via a CCA ligation method. There were several reasons for building those models with this method. First, the rabbit coagulation system was similar to that of humans. Second, the size of rabbit brain vessels was suitable for measurement of cerebrovascular flow rate by Doppler ultrasound, aiding hemodynamic analysis. Most importantly, the models built by CCA ligation were only affected by hemodynamic changes, excluding interferences from other confounders (e.g. hypertensive agents) and thereby improving the accuracy of hemodynamics in revealing the occurrence of aneurysms. Here we studied the aneurysm animal models built through pure hemodynamic induction *in vivo*, and analyzed the changes of molecular biology due to different hemodynamic changes, facilitating the study on occurrence and metastasis/development mechanisms of hemodynamically induced aneurysm.

As reported, hemodynamically induced aneurysm models showed complex hemodynamic changes at the basilar artery bifurcation postoperatively, and manifested as local high WSS and WSS gradient (WSSG), suggesting such hemodynamic changes might promote the occurrence of aneurysms (15). Further rabbit cervix arterial ligation models showed that the flow rate increase in the UL group was smaller compared to the BL group, but the bifurcation vascular walls suffering destructive remodeling under the impact of blood flow were smaller, thereby eliminating the occurrence of aneurysm. It was believed the occurrence of such aneurysm was closely related to the increase of basilar artery blood flow, and the incidence of aneurysm was dose-dependent and correlated with the degree of blood flow impact. Here the three animal models were tested with Doppler ultrasound, and the results show that the basilar artery flow rate in the Sham group did not change significantly with time, but that in the UL group increased, though at smaller degree than the BL group. The vascular wall remodeling degree at the bifurcation was significantly enhanced, further validating the reliability of this method in simulating aneurysm formation via hemodynamic induction.

Although hemodynamic variation can induce the vascular remodeling at the bifurcation and the subsequent aneurysm formation, its underlying mechanism and molecular signaling pathway are still unknown. Hemodynamic research indicates that during vascular blood flow, vascular endothelial cells are responsive

to hemodynamic change and have direct contact with blood (16). When the bifurcation endures continuous abnormal blood impact, the endothelial cells suffer malignant adaptation accordingly, subjected to expressive changes of some signaling molecules and further inducing pathological reaction in vascular walls. As a result, apoptosis of smooth muscle cells and degradation of internal elastic membranes occur, locally forming thin and weak structures and finally inducing aneurysm.

As reported, the vortex at bending and bifurcation parts can induce abnormal vascular responses and cause different pathophysiological outcomes (17). It is believed that endothelial cells can sense the hemodynamic changes (high wall shear stress), thereby transforming to expression of downstream molecular signals. Recently, a growing number of evidences confirm that KLFs are major regulators of endothelial cell biology (5). KLF2 has been confirmed as the most important one in regulation of endothelial functions (18, 19). KLFs are a family of transcription factors first discovered in *Drosophila*. There are 17 KLFs in mammals regulating the expression of many endothelial cell genes and participating in inflammatory reactions, including the endothelin pathway, NO synthetase regulation pathway, matrix metalloproteinase regulation pathway, and NF- κ B reactivation. These downstream genes and products include majority of the known molecular pathways involved in ICA formation.

IHC staining results of KLF2 showed that the basilar artery tips in the Sham group contained a part of weakly positive endothelial cells, while the positive middle-layer smooth muscle cells were sparsely distributed. In the UL group, besides the enhanced expression of epithelial cells, positive staining also occurred in the middle-layer smooth muscle cells. In the BL group, KLF2 was strongly expressed in all layers after week 1, with significant difference compared to the other two groups. Protein quantitative analysis also showed that KLF2 was only weakly expressed in the Sham group, while the expression level was successively increased in the UL group and the BL group. Such expression change was consistent with the increase of basilar artery blood flow rate. These results indicated that KLF2 expression changed accordingly with the hemodynamic variation, which was accompanied by the occurrence of aneurysm at the basilar artery bifurcation.

The rabbit aneurysm model based on pure hemodynamic induction was built via a common carotid artery ligation method. The hemodynamic change was most significant after bilateral ligation, which was most suitable for building animal models for aneurysm research. KLF2 expression change was consistent with blood flow rate variation, which showed positive correlation, indicating KLF2 expression was regulated by hemodynamic changes.

Acknowledgments

This research was supported by the National Natural Science Foundation of China (Grant No. 81301005).

References

1. Pearson, R., J. Fleetwood, S. Eaton, M. Crossley, and S. Bao, Kruppel-like transcription factors: a functional family. *Int J Biochem*

Cell Biol, 2008, **40**:1996-2001. doi: 10.1016/j.biocel.2007.07.018

2. Wu, J., C.S. Bohanan, J.C. Neumann, and J.B. Lingrel, KLF2 transcription factor modulates blood vessel maturation through smooth muscle cell migration. *J Biol Chem*, 2008, **283**:3942-3950. doi: 10.1074/jbc.M707882200

3. Young, A., W. Wu, W. Sun, H. Benjamin Larman, N. Wang, Y.S. Li, J.Y. Shyy, S. Chien, and G. Garcia-Cardena, Flow activation of AMP-activated protein kinase in vascular endothelium leads to Kruppel-like factor 2 expression. *Arterioscler Thromb Vasc Biol*, 2009, **29**:1902-1908. doi: 10.1161/ATVBAHA.109.193540

4. SenBanerjee, S., Z. Lin, G.B. Atkins, D.M. Greif, R.M. Rao, A. Kumar, M.W. Feinberg, Z. Chen, D.I. Simon, F.W. Lusinskas, T.M. Michel, M.A. Gimbrone, Jr., G. Garcia-Cardena, and M.K. Jain, KLF2 Is a novel transcriptional regulator of endothelial proinflammatory activation. *J Exp Med*, 2004, **199**:1305-1315. doi: 10.1084/jem.20031132

5. Atkins, G.B. and M.K. Jain, Role of Kruppel-like transcription factors in endothelial biology. *Circ Res*, 2007, **100**:1686-1695. doi: 10.1161/01.RES.0000267856.00713.0a

6. Das, H., A. Kumar, Z. Lin, W.D. Patino, P.M. Hwang, M.W. Feinberg, P.K. Majumder, and M.K. Jain, Kruppel-like factor 2 (KLF2) regulates proinflammatory activation of monocytes. *Proc Natl Acad Sci U S A*, 2006, **103**:6653-6658. doi: 10.1073/pnas.0508235103

7. Gdynia, H.J., P. Kuhnlein, A.C. Ludolph, and R. Huber, Connective tissue disorders in dissections of the carotid or vertebral arteries. *J Clin Neurosci*, 2008, **15**:489-494. doi: 10.1016/j.jocn.2007.10.001

8. Connolly, E.S., Jr., T.F. Choudhri, W.J. Mack, J. Mocco, T.J. Spinks, J. Slosberg, T. Lin, J. Huang, and R.A. Solomon, Influence of smoking, hypertension, and sex on the phenotypic expression of familial intracranial aneurysms in siblings. *Neurosurgery*, 2001, **48**:64-68; discussion 68-69.

9. Futami, K., J. Yamashita, O. Tachibana, S. Higashi, K. Ikeda, and T. Yamashita, Immunohistochemical alterations of fibronectin during the formation and proliferative repair of experimental cerebral aneurysms in rats. *Stroke*, 1995, **26**:1659-1664.

10. Lopes, D.K., A.J. Ringer, A.S. Boulos, A.I. Qureshi, B.B. Lieber, L.R. Guterman, and L.N. Hopkins, Fate of branch arteries after intracranial stenting. *Neurosurgery*, 2003, **52**:1275-1278; discussion 1278-1279.

11. Dolan, J.M., H. Meng, F.J. Sim, and J. Kolega, Differential gene expression by endothelial cells under positive and negative stream-wise gradients of high wall shear stress. *Am J Physiol Cell Physiol*, 2013, **305**:C854-866. doi: 10.1152/ajpcell.00315.2012

12. Abe, K., Y. Fujino, A. Demizu, Y. Takauchi, T. Hoshida, K. Kamada, T. Mashimo, and I. Yoshiya, The effect of prostaglandin E1 on local cerebral blood flow during cerebral-aneurysm clip ligation. *Eur J Anaesthesiol*, 1991, **8**:359-363.

13. Yamakado, K., N. Tanaka, T. Nakagawa, S. Kobayashi, M. Yanagawa, and K. Takeda, Renal angiomyolipoma: relationships between tumor size, aneurysm formation, and rupture. *Radiology*, 2002, **225**:78-82. doi: 10.1148/radiol.2251011477

14. Meng, H., V.M. Tutino, J. Xiang, and A. Siddiqui, High WSS or low WSS? Complex interactions of hemodynamics with intracranial aneurysm initiation, growth, and rupture: toward a unifying hypothesis. *AJNR Am J Neuroradiol*, 2014, **35**:1254-1262. doi: 10.3174/ajnr.A3558

15. Meng, H., Z. Wang, Y. Hoi, L. Gao, E. Metaxa, D.D. Swartz, and J. Kolega, Complex hemodynamics at the apex of an arterial bifurcation induces vascular remodeling resembling cerebral aneurysm initiation. *Stroke*, 2007, **38**:1924-1931. doi: 10.1161/STROKEAHA.106.481234

16. Chiu, J.J. and S. Chien, Effects of disturbed flow on vascular endothelium: pathophysiological basis and clinical perspectives. *Physiol Rev*, 2011, **91**:327-387. doi: 10.1152/physrev.00047.2009

17. Zaragoza, C., C. Gomez-Guerrero, J.L. Martin-Ventura, L. Blanco-Colio, B. Lavin, B. Mallavia, C. Tarin, S. Mas, A. Ortiz, and J. Egido, Animal models of cardiovascular diseases. *J Biomed Biotechnol*, 2011, **2011**:497841. doi: 10.1155/2011/497841

18. Nakajima, N., S. Nagahiro, T. Sano, J. Satomi, Y. Tada, K. Yagi, K.T. Kitazato, and K. Satoh, Kruppel-like zinc-finger transcription factor 5 (KLF5) is highly expressed in large and giant unruptured cerebral aneurysms. *World Neurosurg*, 2012, **78**:114-121. doi:

10.1016/j.wneu.2011.05.052

19. Ali, M.S., R.M. Starke, P.M. Jabbour, S.I. Tjounakaris, L.F. Gonzalez, R.H. Rosenwasser, G.K. Owens, W.J. Koch, N.H. Greig, and A.S. Dumont, TNF-alpha induces phenotypic modulation in cerebral vascular smooth muscle cells: implications for cerebral aneurysm pathology. *J Cereb Blood Flow Metab*, 2013, **33**:1564-1573. doi: 10.1038/jcbfm.2013.109